

# Tilted Plane Feldkamp Type Reconstruction Algorithm for Spiral Cone-beam CT

Ming Yan Cishen Zhang

School of Electrical and Electronic Engineering,  
Nanyang Technological University,  
Nanyang Avenue, Singapore 639798.  
Email: [yanming@pmail.ntu.edu.sg](mailto:yanming@pmail.ntu.edu.sg)

## Abstract

An approximation image reconstruction method for spiral cone-beam computed tomography (CT), called Tilted Plane Feldkamp Type Reconstruction Algorithm (TPFR), is presented in this paper, which extends the Feldkamp cone-beam reconstruction algorithm to overcome its inaccuracy problem caused by large cone-angle. This is done by tilting the reconstructing planes to minimize the cone angle and optimally fit the spiral segment of the source. After reconstruction of tilted plane images, a subsequent interpolation step reforms the tilted plane images to plane images perpendicular to the z-axis. Simulations of Shepp-Logan phantom can show that the image reconstruction performance of the proposed TPFR algorithm is superior to that of the conventional Feldkamp type reconstruction algorithm.

## 1 Introduction

Spiral CT introduced in early 1990s and the development of multi-slice computed tomography (MSCT) in 1998 brought together improved capability and enabled rapid scanning of a large volume of object in short time in CT. Owing to the improved volume scanning speed, new clinical applications of CT with high image quality and using multidimensional algorithms are under continuous development.

There have been a number of early algorithms for MSCT reconstruction for low number of detector rows [1,2,3]. These algorithms assume that projection rays measured on different detector rows are parallel to each other and perpendicular to the longitudinal axis. A complete set of projection data for reconstruction can be formed by interpolation in the longitudinal direction. These can be classified as 360° Linear Interpolation algorithm and 180° Linear Interpolation algorithm. Because these algorithms do not take into account the effects of cone angle, severe cone-beam artifacts may occur when the number of detector rows is large.

A number of algorithms have been proposed to deal with the reconstruction problem for MSCT with large number of detector rows. These algorithms are classified into two major categories: exactly algorithms [4-8] and approximation algorithms.

The approximation algorithms can be divided into 2-dimensional (2D) and 3-dimensional (3D) algorithms. Popular 2D approximation algorithms are known as: ASSR [9], AMPR [10,11] and GSR [12]. ASSR and AMPR algorithms use the tilted reconstruction planes and GSR algorithm uses the optimal surface to minimize the cone angle to reduce artifacts.

The most well known 3D approximation algorithm is Feldkamp algorithm [13] which extends the 2D fan-beam filtered back projection algorithm to the 3D reconstruction to provide feasible and efficient parallel processing. However, it has a major drawback in artifacts caused by large cone angle when the reconstruction plane is far from the centre plane. To deal with this difficulty, a spiral trajectory is introduced in [14] and interpolation and shot-scan methods are employed in [15] for reduction of artifacts of the Feldkamp type algorithm. The algorithm in [15] is further modified in [16] for gantry-tilted reconstruction.

The TPFR algorithm proposed in this paper uses tilted reconstruction planes to optimally fit the source trajectory. This adaptively minimizes the cone angle with respect to different pitch and slice-thickness so as reducing artifacts caused by the large cone angle.

Section 2 forms the optimal tilted reconstruction planes. Section 3 presents coordinate systems and transformations between them for the TPRF algorithm. In Section 4, the equal-angular Feldkamp type filtered backprojection equation is presented followed by the TPRF reconstruction procedure and formulas. Simulation results of TPRF algorithm are presented in Section 5.

## 2 Tilted reconstruction plane

With respect to the in-plane coordinate system in Fig. 1 and the scanning geometry of spiral cone beam CT in Fig. 2, the following notations and definitions are used throughout the paper.

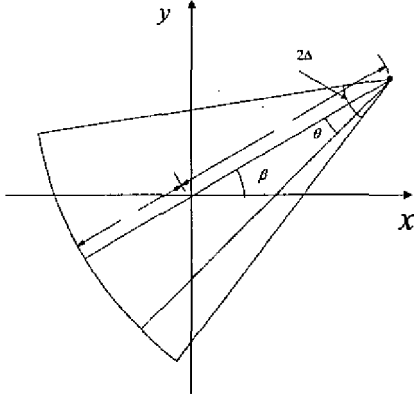


Fig 1. In-plane coordinate system for cone-beam spiral CT.

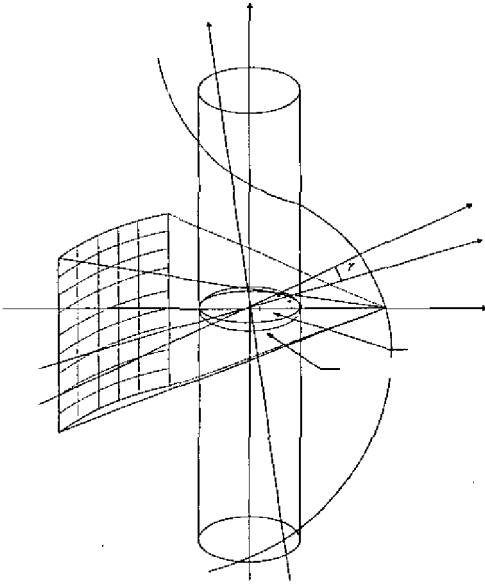


Fig 2. Scanning geometry of the cone-beam spiral CT, where the spiral line is the source trajectory, the normal plane is perpendicular to the z-axis and the plane encircled by the dotted circle line is the tilted plane.

- $x-y-z$  the global coordinate system;
- $P_i$  the tilted reconstruction plane
- $R_f$  the source-isocenter distance;
- $R_d$  the isocenter-detector distance;

- $p$  the pitch;
- $S$  slice-thickness;
- $2\Delta$  the fan angle;
- $M$  number of the detector slices;
- $\theta$  the projection angle within the fan;
- $\beta$  the fan-beam projection angle;
- $\beta_p$  the centre projection angle of the tilted reconstruction plane;
- $\gamma$  tilted angle of the reconstruction plane with respect to the  $x-y$  plane;
- $z_p$  the centre position of the tilted reconstruction plane in  $z$ -direction;
- $z_{ini}$  the initial position of the source in the  $z$ -direction;
- $\xi-\eta-\zeta$  the local coordinate system formed by rotating the  $x-y-z$  coordinate system by  $\beta_p$  around  $z$ -axis,  $\xi = \xi(\beta_p)$ ,  $\eta = \eta(\beta_p)$ ,  $\zeta = z$ ;
- $x'-y'-z'$  the local coordinate system formed by rotating the  $\xi-\eta-\zeta$  coordinate system by  $\gamma$  around  $\xi$ -axis,  $x' = \xi$ ,  $y' = \eta(\gamma)$ ,  $z' = z'(\gamma)$ ;
- $s-t-z$  the local coordinate system by rotating the  $x-y-z$  coordinate system by  $\beta$  around  $z$ -axis.
- $D(\beta, \theta)$  projection data from the detector

The proposed TPF algorithm constructs image of the tilted plane  $P_i$  which has the tilted angle  $\gamma$  and the centre projection angle  $\beta_p$ . The algorithm uses half scan with the projection angle

$$\beta \in [\beta_p - (\pi + 2\Delta)/2, \beta_p + (\pi + 2\Delta)/2]$$

Let  $s(\beta)$  be the source trajectory which is a function of  $\beta$  and is given by

$$s(\beta) = \begin{pmatrix} R_f \cos \beta \\ R_f \sin \beta \\ z_{ini} + \frac{pSM\beta}{2\pi} \end{pmatrix} \quad (1)$$

The intersection of the tilted plane  $P_i$  with the cylinder of the source trajectory is also a function of  $\beta$  which is denoted by  $e(\beta)$  and given by the following ellipse:

$$e(\beta) = \begin{pmatrix} R_f \cos \beta \\ R_f \sin \beta \\ z_p + R_f \tan \gamma \sin(\beta - \beta_p) \end{pmatrix} \quad (2)$$

The motivation the TPF algorithm in dealing with the cone beam artifacts of the Feldkamp algorithm is to minimize the mean square error between the source trajectory  $s(\beta)$  and the ellipse  $e(\beta)$  in the  $z$ -direction. It

follows from (1) and (2) that the distance between  $s(\beta)$  and  $e(\beta)$  is:

$$\begin{aligned} & z_{im} + \frac{pSM\beta}{2\pi} - z_p - R_f \tan \gamma \sin(\beta - \beta_p) \\ = & z_{im} + \frac{pSM\beta}{2\pi} - z_{im} - \frac{pSM\beta_p}{2\pi} - R_f \tan \gamma \sin(\beta - \beta_p) \\ = & \frac{pSM(\beta - \beta_p)}{2\pi} - R_f \tan \gamma \sin(\beta - \beta_p) \end{aligned} \quad (3)$$

For  $\beta \in [\beta_p - (\pi + 2\Delta)/2, \beta_p + (\pi + 2\Delta)/2]$ , let

$$\bar{\beta} = (\beta - \beta_p) \in [-(\pi + 2\Delta)/2, (\pi + 2\Delta)/2]$$

Using (3), the least mean square error between  $s(\beta)$  and  $e(\beta)$  in the z-direction is given by

$$J^2(\gamma) = \int_{-(\pi+2\Delta)/2}^{(\pi+2\Delta)/2} (R_f \tan \gamma \sin \bar{\beta} - pSM\bar{\beta}/2\pi)^2 d\bar{\beta} \quad (4)$$

It can be computed that

$$J^2(\gamma) = A \tan^2 \gamma - B \tan \gamma + C \quad (5)$$

where

$$A = R_f^2 (\beta_m + \sin \beta_m \cos \beta_m)$$

$$B = (\sin \beta_m - \beta_m \cos \beta_m) R_f pSM / \pi$$

$$C = p^2 S^2 M^2 \beta_m^3 / (6\pi^2)$$

$$\beta_m = (\pi + \Delta) / 2$$

It turns out that the optimal  $\gamma$  which minimizes the mean square error function  $J(\gamma)$  in (4) and (5) is given by

$$\gamma = \tan^{-1}(B/2A) \quad (6)$$

This provides a formula for determining and computing the angle of the tilted image reconstruction plane in the TPFPR algorithm.

### 3 Coordinate system transformations

The proposed TPFPR algorithm reconstructs the image of the tilted plane by rotating the coordinate system such that the conventional Feldkamp reconstruction algorithm can be extended the tilted plane  $P_r$ . We now present coordinate system transformations for representing equations for the tilted plane with respect to the source and detector. The

local coordinate system  $\xi$ - $\eta$ - $\zeta$  is given by rotating the global coordinate system  $x$ - $y$ - $z$  by  $\beta_p$  about the z-axis, i.e.

$$\begin{pmatrix} \xi \\ \eta \\ \zeta \end{pmatrix} = \begin{pmatrix} \cos \beta_p & \sin \beta_p & 0 \\ -\sin \beta_p & \cos \beta_p & 0 \\ 0 & 0 & 1 \end{pmatrix} \begin{pmatrix} x \\ y \\ z \end{pmatrix} = T_{\beta_p} \begin{pmatrix} x \\ y \\ z \end{pmatrix} \quad (7)$$

Further rotating the local coordinate system  $\xi$ - $\eta$ - $\zeta$  by  $\gamma$  around the  $\xi$ -axis yields the tilted local coordinate system  $x'$ - $y'$ - $z'$  as follows.

$$\begin{pmatrix} x' \\ y' \\ z' \end{pmatrix} = \begin{pmatrix} 1 & 0 & 0 \\ 0 & \cos \gamma & \sin \gamma \\ 0 & -\sin \gamma & \cos \gamma \end{pmatrix} \begin{pmatrix} \xi \\ \eta \\ \zeta \end{pmatrix} = T_\gamma \begin{pmatrix} \xi \\ \eta \\ \zeta \end{pmatrix} \quad (8)$$

On the tilted reconstruction plane  $P_r$ , the origin  $o'$  of  $P_r$  in the  $x$ - $y$ - $z$  coordinate system is given by

$$o' = \begin{pmatrix} 0 \\ 0 \\ z_{im} + pSM \frac{\beta_p}{2\pi} \end{pmatrix}$$

Thus we can obtain an equation for the tilted reconstruction plane  $P_r$  in the  $x$ - $y$ - $z$  coordinate system as

$$z = -x \sin \beta_p \tan \gamma + y \cos \beta_p \tan \gamma + z_{im} + pSM \frac{\beta_p}{2\pi} \quad (9)$$

Because the tilted plane  $P_r$  is perpendicular to the  $z'$ -axis in the  $x'$ - $y'$ - $z'$  coordinate system, the equiangular Feldkamp type half-scan algorithm is applicable for reconstructing the tilted plane  $P_r$ .

In the local coordinate system  $x'$ - $y'$ - $z'$ , the source position, denoted by  $s' = (x_s', y_s', z_s')^T$  is

$$s' = \begin{pmatrix} x_s' \\ y_s' \\ z_s' \end{pmatrix} = T_{\beta_p} T_\gamma \begin{pmatrix} R_f \cos \beta \\ R_f \sin \beta \\ z_{im} + pSM \frac{\beta}{2\pi} \end{pmatrix}$$

where  $T_{\beta_p}$  and  $T_\gamma$  are as defined in (7) and (8), respectively, and the source-isocenter distance  $R_f$  is fixed in the  $x$ - $y$ - $z$  coordinate system. The source-isocenter distance  $R_f'$  in the  $x'$ - $y'$ - $z'$  coordinate system is

$$R_f' = \sqrt{x_s'^2 + y_s'^2} \quad (10)$$

With respect to the projection angle  $\beta$  in the  $x$ - $y$ - $z$  coordinate system, the corresponding projection angle in the  $x'$ - $y'$ - $z'$  coordinate system, denoted as  $\beta'$ , is

$$\beta' = \begin{cases} 3\pi/2, & x_s' = 0, y_s' < 0 \\ 5\pi/2, & x_s' = 0, y_s' > 0 \\ 3\pi + a \tan(x_s' / y_s'), & x_s' / y_s' < 0, \beta > 5\pi/2 \\ \pi + a \tan(x_s' / y_s'), & x_s' / y_s' > 0, \beta < 3\pi/2 \\ \pi \tan(x_s' / y_s') + 2\pi, & \text{otherwise} \end{cases} \quad (11)$$

In the  $x'$ - $y'$ - $z'$  coordinate system and with respect to the projection angle  $\beta'$ , any point on the detector plane, denoted as,  $D_{\beta'}(i, j)$  can be represented as

$$D_{\beta'}(i, j) = \begin{pmatrix} x_p' \\ y_p' \\ z_p' \end{pmatrix} = \begin{pmatrix} R_f' \cos(\pi + \bar{\theta} + \beta') + x_s' \\ R_f' \sin(\pi + \bar{\theta} + \beta') + y_s' \\ (j - (M - 1)/2)S \end{pmatrix} \quad (12)$$

where  $\bar{\theta} = -\Delta + i\theta_d$  is the fan angle in the  $x'$ - $y'$ - $z'$  and  $\theta_d$  is an angular increment of the projection angle in the fan beam. Let  $D_{\beta}(m, n)$  denote the  $x$ - $y$ - $z$  coordinate system representation of the detector point  $D_{\beta'}(i, j)$ . It can be written as

$$D_{\beta}(m, n) = \begin{pmatrix} x_p \\ y_p \\ z_p \end{pmatrix} = \begin{pmatrix} \cos \beta_p & -\sin \beta_p & 0 \\ \sin \beta_p & \cos \beta_p & 0 \\ 0 & 0 & 1 \end{pmatrix} \begin{pmatrix} 1 & 0 & 0 \\ 0 & \cos \gamma & -\sin \gamma \\ 0 & \sin \gamma & \cos \gamma \end{pmatrix} \begin{pmatrix} x_p' \\ y_p' \\ z_p' \end{pmatrix} \quad (13)$$

The detector point  $D_{\beta}(m, n)$  is indexed by three parameters, the angular position index  $\beta$ , the detector row index  $n$  and detector column index  $m$ . These indices identify the projection data from the projection dataset.

The coordinate system  $s$ - $t$ - $z$  is a rotation of the  $x$ - $y$ - $z$  coordinate system by  $\beta$  around  $z$ -axis such that

$$s = x \sin \beta + y \cos \beta, \quad t = -x \sin \beta + y \cos \beta, \quad z = z$$

Given  $x_p, y_p$  and  $\beta$ , the corresponding point  $(s_p, t_p)$  of  $D_{\beta}(m, n)$  in the  $s$ - $t$ - $z$  coordinate system is given by

$$s_p = x_p \cos \beta + y_p \sin \beta \quad t_p = -x_p \sin \beta + y_p \cos \beta$$

With respect to the  $s$ - $t$ - $z$  coordinate system, the indices  $n$  and  $m$  can be computed from

$$n = \text{mod} \left[ \left( \frac{R_f(z_p - z_f)}{R} + (M - 1)S/2 \right) / S \right] \quad (14)$$

$$R = \sqrt{(x \cos \beta - R_f \cos \beta)^2 + (y \sin \beta - R_f \sin \beta)^2}$$

$$m = \text{mod} \left[ \left( \tan^{-1} \left( \frac{-R_f t_p}{R_f - s_p} \right) + \Delta \right) / \theta_d \right] \quad (15)$$

where  $z_f = z_{m0} + pSM\beta/2\pi$  is the source in the  $z$ -direction.

With the coordinate system transformations from the original coordinate system  $x$ - $y$ - $z$  as given above, the projection data set of the tilted coordinate system which is determined by  $\gamma$  and  $\beta_p$  can be obtained. Based on the projection data set, the image of the tilted plane can be reconstructed by applying the conventional Feldkamp algorithm which is presented in the following section.

#### 4 Equal-angular Feldkamp Type Half-scan backprojection

The conventional Equal-angular Feldkamp Type backprojection algorithm can be written as

$$f(x, y, z) = \int_0^{2\Delta} \frac{1}{r^2} \int_{-s_2}^{s_2} R(\beta, \theta, k) W(\beta, \theta) g(\theta - \theta_d) d\theta d\beta \quad (16)$$

where

$$R(\beta, \theta, k) = D(\beta, \theta, k) R_f \cos \theta$$

$D(\beta, \theta, k)$  represents the projection data collected from the detector,  $k = \text{mod}((z_d + (M - 1)S/2)/S)$  is the detector column index with

$$z_d = \frac{R_f(z - z_f)}{R}$$

$$R = \sqrt{(x \cos \beta - R_f \cos \beta)^2 + (y \sin \beta - R_f \sin \beta)^2}$$

for the reconstruction plane,  $z$  is defined in (9),  $z_f$  is the position of the source in the  $z$ -direction defined by (1),  $W(\beta, \theta)$  is the weighting factor of the shot-scan algorithm [17] written as

$$W(\beta, \theta) = \begin{cases} \sin^2 \left( \frac{\pi \beta}{4\Delta - \theta} \right) & 0 \leq \beta \leq 2\Delta - 2\theta \\ 1 & 2\Delta - 2\theta \leq \beta \leq \pi - 2\Delta \\ \sin^2 \left( \frac{\pi \pi + 2\Delta - \beta}{4\Delta + \theta} \right) & \pi - 2\Delta \leq \beta \leq \pi + 2\Delta \end{cases}$$

and  $g(\theta' - \theta)$  is the ramp-filter with

$$\theta' = \tan^{-1} \left( \frac{-R_f t}{R_f^2 - \sqrt{R_f^2 - z_d^2} s} \right)$$

Let  $L = \sqrt{(R_f^2 + z_d^2)(R_f - s)^2 + R_f^2 t^2} / R_f$  be the distance from the source to the point  $(x, y, z)$ . The reconstruction formula also can be written as :

$$f(x, y, z) = \int_{\beta}^{\beta+2\Delta} \frac{1}{L^2} Q_{\beta} \left( \tan^{-1} \left( \frac{-R_f t}{R_f^2 - \sqrt{R_f^2 - z_d^2} s} \right), \frac{R_f(z - z_f)}{R} \right) d\beta$$

where  $Q_{\beta}(\theta', k) = [R(\beta, \theta, k)W(\beta, \theta)] * g(\theta)$

The tilted plane reconstruction procedure is to reconstruct the image of the tilted plane  $P_t$  by applying the conventional Equal-angular Feldkamp Type back projection algorithm to the tilted coordinate system  $x'-y'-z'$ . The tilted plane reconstruction can follow the following procedure.

1. Determine a  $\beta_p$  and calculate optimal tilted angle  $\gamma$  with (6);
2. For each  $\beta \in \{\beta_p - (\pi + 2\Delta)/2, \beta_p - (\pi + 2\Delta)/2\}$ ,
  - Calculate  $\beta'$  using (11)
  - Calculate  $R'_j$  using (10)
  - Calculate the projection data  $D'_p(i, j)$  in the tilted coordinate system  $x'-y'-z'$  by calculating  $n$  and  $m$  using (14) and (15) with  $D'_p(i, j) = D_p(m, n)$  in the global coordinate system  $x-y-z$ .
3. With the projection dataset of the tilted coordinate system getting from former step, we can reconstruct the plane  $P_t$  defined by (9) with reconstruction equation (16).

Reconstructed tilted plane images are then used to form images for planes perpendicular to the  $z$ -axis by interpolation. This is carried out by the following interpolation formula:

$$f_z(x, y) = \frac{\sum_{i=1}^2 |z_i - z| f(x, y, z_i)}{|z_1 - z_2|}$$

where  $z_1(x, y)$  and  $z_2(x, y)$  are two points on different images which are most adjacent to the specified  $z$ -position at  $(x, y)$ .

## 5 Simulation and Results

We evaluate the proposed TPFR algorithm by reconstruction of simulated raw data of Shepp-Logan

phantom. The simulation parameters were chosen as  $M=16$ ,  $S=1\text{mm}$  with 512 detector channels per row,  $R_f=570\text{mm}$ ,  $R_d=300\text{mm}$  and  $p=0.8, 1.0$  and  $1.2$  respectively. Tilted images were reconstructed at an increment of  $S/4$ .

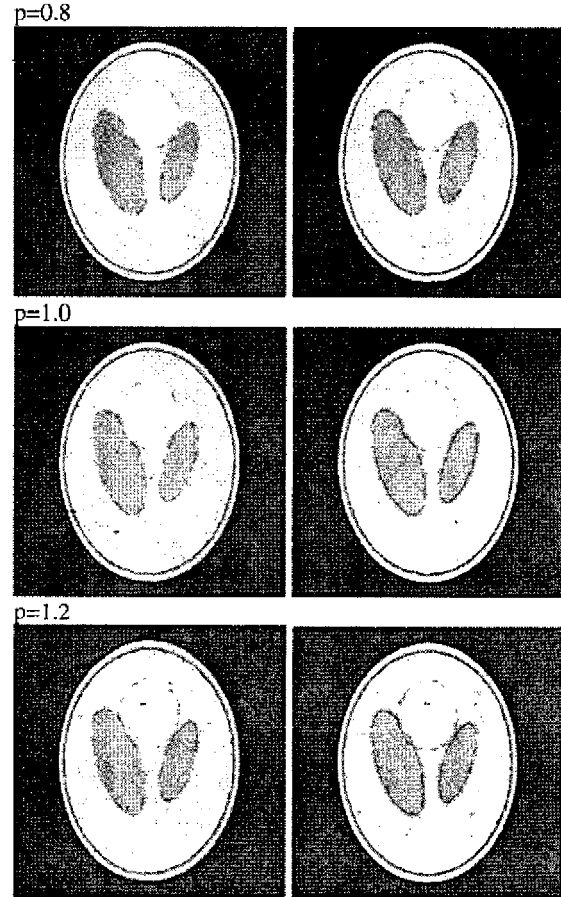


Fig 3. Image reconstruction of the Shepp-Logan phantom at different pitches. Images in the left column are reconstructed by conventional Feldkamp algorithm and that of the right column are by TPFR algorithm.

The simulated performance of the TPFR algorithm and its comparison with the conventional Feldkamp algorithm are shown in Fig 3, where figures in the left column are images reconstructed by the conventional Feldkamp algorithm and that in the right column are images reconstructed by TPFR algorithm. It is shown that the two small ellipsoids in the bottom part of the left side images become blurred as the table increment increases. In contrast, the corresponding small ellipsoids in the images reconstructed by TPFR algorithm in the right column are clearly shown. These results demonstrate that the TPFR

algorithm can greatly reduce visible cone-beam artifacts in reconstructed images and improve the image quality.

## 6 Conclusions

In multi-slice spiral CT image reconstruction, it is important to take into account the cone-angle of the rays when the number of slice exceeds a certain threshold and the existing Feldkamp algorithm suffers from large inaccuracy when the cone-angle is large. The tilted reconstruction plane of proposed TPF algorithm can optimally fit the spiral source trajectory to minimize cone beam artifacts. Its computing procedure is simple and its advantages in image reconstruction are demonstrated by simulations.

## References

- [1] K. Taguchi and H. Aradate, "Algorithm for image reconstruction in multi-slice helical CT," *Med. Phys.* Vol. 25, No. 4, 550-561, 1998.
- [2] H. Hu, "Multi-slice helical CT: Scan and reconstruction," *Med. Phys.* Vol. 26, No.1, 5-18, 1999.
- [3] S. Schaller, T. Flohr, K. Klingenberg, J. Krause, T. Fuchs, and W. A. Kalender, "Spiral interpolation algorithm for multislice spiral CT-Part I: Theory," *IEEE Trans. Med. Imag.* Vol.19, No. 9, 822-834, 2000.
- [4] H. K. Tuy, "An inversion formula for cone-beam reconstruction," *SIAM J. Appl. Math.*, Vol.43, no. 3, 546-562, 1983
- [5] B. D. Smith, "Image reconstruction from cone-beam projections: Necessary and sufficient conditions and reconstruction methods," *IEEE Trans. Med. Imag.*, vol. MI-4, 14-25, 1985.
- [6] H. Kudo, F. Noo, and M. Defrise, "Cone beam filtered-backprojection algorithm for truncated helical data," *Phys. Med. Biol.*, Vol. 43, 2885-2909, 1998.
- [7] R. Proksa, Th. Köhler, M. Grass, and J. Timmer, "The n-PI-Method for Helical Cone-Beam CT," *IEEE Trans. Med. Imag.* Vol. 19, No. 9, 848-863, 2000.
- [8] M. Defrise, F. Noo, and H. Kudo, "A solution to the long object problem in helical cone-beam tomography," *Phys. Med. Biol.*, Vol. 45, 1-21, 2000.
- [9] M. Kachelrieß, S. Schaller, W.A. Kalender, "Advanced single slice rebinning in cone-beam spiral CT," *Med. Phys.* Vol. 27, No. 4, 754-772, 2000.
- [10] S. Schaller, K. Stierstorfer, H. Bruder, M. Kachelrieß, and T. Flohr, "Novel approximate approach for high-quality image reconstruction in helical cone beam CT at arbitrary pitch," *Proc. SPIE* 4322, 113-127, 2001.
- [11] Th. Flohr, K. Stierstorfer, H. Bruder, J. Simon, A. Polacin, and S. Schaller, "Image reconstruction and image quality evaluation for a 16-slice CT scanner," *Med. Phys.* Vol. 30, No. 5, 832-844, 2003.
- [12] L. Chen, Y. Liang, D. J. Heuscher, "General surface reconstruction for cone-beam multislice spiral computed tomography", *Med. Phys.* Vol. 30, No.10, 2804-2821, 2003
- [13] L. A. Feldkamp, L. C. Davis, and J. W. Kress, "Practical cone-beam algorithm," *J. Opt. Soc. Am. A* 1, 612-619, 1984.
- [14] G. Wang, T. Lin, P. Cheng, D. M. Schiozaki, "A General Cone-Beam Reconstruction Algorithm", *IEEE Transactions on Medical Imaging*, Vol, 12, No.3, 486-496, 1993.
- [15] Mori and T. Suzuki, "Development of advanced multislice CT scanner Aquilion," *Med. Rev.* 78, 1-7, 2001.
- [16] I. Hein, K. Taguchi, M. D. Silver, M. Kazama, I. Mori, "Feldkamp-based cone-beam reconstruction for gantry-tilted helical multislice CT," *Med. Phys.* Vol. 30, No. 12, 3233-3242, 2003.
- [17] D. L. Parker, "Optimal short scan convolution reconstruction for fan beam CT," *Med. Phys.* Vol. 9, No.9, 254-257, 1982.